

are in poor agreement with bonding schemes which consider only two of the four valence orbitals as bonding orbitals. In particular, the hybridized bonding scheme proposed by Stewart, as well as two unhybridized bonding schemes, yields poor agreement with the experimental NQCC unless (d-p)  $\pi$ -bonding (or hyperconjugation) is postulated. (4) Calcium coordination to the diopside bridging oxygen is consistent with calcium in a charge acceptor role. The results are consistent with McDonald's (d-p)  $\pi$ -bonding model. (5) Analysis of the NQCC of bridging oxygen bonded to elements other than silicon in well-defined systems further evidences the usefulness of the Pauling orbital occupancies in tandem with the Townes-Dailey treatment as a predictive tool for oxygen NQCC. (6) The dependence of the  $^{17}\text{O}$  NQCC in the  $\text{SiO}_2$  polymorphs as a function of bridging angle may yield insight concerning the structural significance of the (d-p)  $\pi$ -bonding effect. (7) Orbital occupancies obtained from Gordy's method yield poor agreement with experiment. (8) The oxygen NQCC are shown consistent with the halide NQCC of analogous systems.

(9) Trends in the oxygen and halide NQCC, of compounds with analogous chemical composition, support the conclusions of (d-p)  $\pi$ -bonding or hyperconjugation in silicates, on electronegativity grounds. (10) Considerable potential exists for use of the NQCC in conjunction with more sophisticated molecular orbital calculations, as well as X-ray electron density maps.<sup>97</sup> Furthermore, as we have previously noted, the (d-p)  $\pi$ -bonding effect may influence the silicon-29 NMR isotropic chemical shift.<sup>98</sup>

**Acknowledgment.** We thank R. J. Kirkpatrick and Gary Turner for helpful discussion. We gratefully acknowledge the help of (the late) Eldon Boatz for his help in producing the figures in this, and many previous, publications.

**Registry No.** Si, 7440-21-3;  $\text{O}_2$ , 7782-44-7;  $^{17}\text{O}$ , 13968-48-4.

(97) Schwarzenbach, D.; Thong, N. *Acta Crystallogr.* **1979**, *A35*, 652.  
(98) Janes, N.; Oldfield, E. *J. Am. Chem. Soc.* **1985**, *107*, 6769.

## Demonstration and Characterization of Two Complexes of Cobalt(II) to Mononucleotides by $^{31}\text{P}$ and $^1\text{H}$ NMR

Jean Louis Leroy and Maurice Guéron\*

*Contribution from the Groupe de Biophysique du Laboratoire<sup>†</sup> de Physique de la Matière Condensée, Ecole Polytechnique, 91128 Palaiseau, France. Received February 4, 1986*

**Abstract:** Direct observation, under slow-exchange conditions, of the  $^{31}\text{P}$  and  $^1\text{H}$  spectra of 5'-AMP in solutions containing  $\text{Co}^{2+}$  demonstrates the existence of at least two different complexes in a temperature-dependent equilibrium. The majority species at low temperature (80% of  $-10^\circ\text{C}$ ) has a small phosphorus paramagnetic shift,  $-48$  ppm, and a large H8 paramagnetic shift,  $-203$  ppm. This indicates indirect coordination to phosphate and direct coordination to N7. This is the same coordination as in the crystals of 5'-monophosphates of purines complexed with transition-metal ions of the first series. The second complex, a 20% minority at  $-10^\circ\text{C}$ , has a large phosphorus shift,  $-2530$  ppm, and a small but significant shift of H8,  $-37$  ppm. This indicates direct coordination to phosphate and suggests indirect coordination to N7. The properties of this complex are in agreement with those of the high-temperature complex, long known from studies in the fast-exchange regime. As a function of temperature, slow and fast exchange regimes are encountered. At some temperatures, one complex is responsible for most of the paramagnetic shift, whereas transverse relaxation is due to the other. The two-complex model fits the  $^{31}\text{P}$  data over the entire temperature range. Thermodynamic and kinetic parameters of the complexes are derived. At  $22^\circ\text{C}$ , their concentrations are equal and the lifetimes are  $15\ \mu\text{s}$  for the first and  $10\ \mu\text{s}$  for the second. The complexation of 5'-CMP with cobalt presents similar properties. The two complexes are octahedral, in contrast to the tetrahedral structure observed in crystals. At least five complexes of Co-5'-ATP are observed on the  $^{31}\text{P}$  spectrum at  $-10^\circ\text{C}$ . Together with prior work on the association of manganese to polynucleotides, the present results suggest that the temperature-dependent equilibrium between indirect and direct metal-to-phosphate ligation could be a rather general feature among transition metals of the first series.

The interaction of divalent ions with nucleotides has been extensively studied. The nitrogen and oxygen donor groups of the bases, the phosphate group, and the ribose hydroxyls are potential binding sites for metal ions. Metal binding is further complicated by the alternative possibilities of direct or indirect (i.e., through a water molecule) ligation and by possible intermolecular metal bonds leading to dimerisation or macrochelate formation.<sup>1,2</sup>

Transition-metal ions such as Ni, Mn, and Co have been widely used as substitutes for the natural Mg ions in kinetic and structural studies by NMR, X-ray diffraction, temperature-jump, and IR spectroscopy techniques.

A survey of metal-nucleotide crystal structures is given by Swaminathan and Sundaralingam.<sup>3</sup> Despite the large variety of cases, this survey reveals some systematic features:

(a) All crystal structures of purine 5'-monophosphate complexes with the transition ions of the first series (Co-IMP, Co-GMP,

Mn-IMP, Mn-GMP, Ni-AMP, Ni-IMP, Ni-AMP, Ni-GMP) share the following properties: (i) the formula is  $[\text{M}^{2+}(\text{NMP})(\text{H}_2\text{O})_5]$ ; (ii) the structure is octahedral; and (iii) the metal ion is coordinated directly to N7 and binds through water to phosphate.

(b) The crystal structures of three pyrimidine-5'-monophosphate complexes of cobalt and manganese ( $\text{Co}_2(5'\text{-UMP})_2(\text{H}_2\text{O})_4$ ,  $\text{Co}(5'\text{-CMP})(\text{H}_2\text{O})$ , and  $\text{Mn}(5'\text{-CMP})(\text{H}_2\text{O})$ ) are known. They are polymeric and the metal ion is coordinated to the oxygens of two different phosphate groups. In Co-5'-CMP,  $\text{Co}^{2+}$  coordinates in addition to the nitrogen N3 of a third CMP molecule,<sup>4</sup> a feature

(1) Martin, R. B.; Yitbareck, H. M. In *Metal Ions in Biological Systems*; Sigel, H., ed. Marcel Dekker: New York, 1979; Vol. 8, Chapter 2, pp 57-124.

(2) Gellert, R. W.; Bau, B. In *Metal Ions in Biological Systems*; Sigel, H., Ed.; Marcel Dekker: New York, 1979; Vol. 8, Chapter 1, pp 1-55.

(3) Swaminathan, V.; Sundaralingam, M. *Crit. Rev. Biochem.* **1979**, *6*, 245-336.

(4) Clark, G. G.; Orbell, J. D. *J. Chem. Soc., Chem. Commun.* **1975**, 697-698.

\* To whom correspondence should be addressed.

<sup>†</sup>Unité de Recherche Associée au Centre National de la Recherche Scientifique.

found in many complexes of cytidine.<sup>2</sup> For this compound only, the cobalt coordination is tetrahedral.

The characterization of the solution complexes is far less advanced. Among the most studied complexes are those of Co-5'-AMP and Mn-5'-AMP. Their coordination mode and kinetics of formation have been studied by the effect of the paramagnetic ion on the <sup>31</sup>P,<sup>5-7</sup> <sup>1</sup>H, <sup>13</sup>C, and <sup>15</sup>N<sup>7</sup> NMR spectra.

Experiments carried out at low metal-to-nucleotide ratio and in the fast exchange regime give evidence for direct coordination of metal to phosphate in these complexes, in contrast to the crystal structures described above. However, such experiments cannot rule out the existence of more than one complexation mode. The difference between complexation modes found in the crystal and in solution, as well as some observations on interactions between manganese and polynucleotides,<sup>8</sup> suggested that there might indeed be more than one complexation mode in solution.

To approach this problem, we attempted to observe directly the NMR spectra of a cobalt-5'-AMP complex. We obtained the phosphorus spectrum of such a complex, between -10 and +5 °C.<sup>9</sup> It was clearly different from the one that could have been expected on the basis of the fast exchange studies carried out at higher temperatures.

We now present a study of the complexes of cobalt with 5'-AMP and 5'-CMP by <sup>1</sup>H and <sup>31</sup>P NMR. We demonstrate the change in complexation mode as a function of temperature and propose models for the complexes.

The choice of the cobalt ion is one of convenience. Due to the short electron spin relaxation time of Co<sup>II</sup>, intrinsic line widths (excluding chemical exchange) are expected to be in many cases smaller than the paramagnetic shifts, which can then be observed.

The purpose and, we hope, usefulness of this work is as a precise illustration of situations that may arise in the study of complexes of metal ions with nucleic acids (monomeric or polymeric, oxy or deoxy, single or double stranded).

Polynucleotides are polyelectrolytes, and as such they are surrounded by cations in larger concentrations than the average concentration in the solution. The formation of complexes is thereby favored, but it should otherwise proceed essentially as with mononucleotides.<sup>10</sup> Cobalt binding to polynucleotides also exhibits different complexation modes (in preparation).

## Theory<sup>6</sup>

This section presents the theoretical results required for the interpretation of the experiments.

**(1) The Complex without Chemical Exchange.** The Co<sup>2+</sup> ion in its ground state has  $L = 3$  and  $S = 3/2$ . The non-zero orbital angular momentum leads to fast electronic spin-lattice relaxation and, in a noncubic environment, to anisotropy of the  $g$  factor.

**(a) The Static Complex.** The interaction with a neighboring nuclear spin  $I$  includes a contact contribution, transmitted through chemical bonds, and a dipolar, through-space contribution.

The contact interaction may be split into an isotropic part and another which is traceless and is designated pseudodipolar.

The dipolar interaction may be similarly split. Its isotropic part, designated as pseudocontact, would vanish except for the anisotropy of the  $g$  factor. The interactions are modulated by electronic spin relaxation:  $\tau_e \approx 5 \times 10^{-13}$  s.<sup>11</sup> Their average values, proportional to  $\langle S_z \rangle$ , the average value of the electronic spin, produce paramagnetic shifts of the ligand nuclei. Their modulation creates fluctuating magnetic fields, leading to nuclear relaxation.<sup>12</sup> Longitudinal relaxation of ligand nuclei by Co<sup>2+</sup> is in fact dominated by this effect.

One has, for  $\omega_1 \tau_e \ll 1$

$$1/T_{1M} = D\tau_e[6 + 14/(1 + \omega_e^2 \tau_e^2)] + C\tau_e/(1 + \omega_e^2 \tau_e^2) \quad (1)$$

$$1/T_{2M} =$$

$$D\tau_e[7 + 13/(1 + \omega_e^2 \tau_e^2)] + C\tau_e[1 + 1/(1 + \omega_e^2 \tau_e^2)] \quad (2)$$

where  $\omega_1$  and  $\omega_e$  are the nuclear and electronic resonance frequencies. The  $D$  and  $C$  terms, corresponding to the dipolar and contact interactions, are (MKS units)

$$D = (1/15)S(S+1)(\omega_1/B)^2 g^2 \beta^2 / (4\pi\epsilon_0 c^2 r^3)^2 \quad (3)$$

$$C = (1/3)S(S+1)(A/\hbar)^2 \quad (4)$$

where  $\beta$  is the Bohr magneton,  $4\pi\epsilon_0 c^2 = 10^7$ ,  $B$  is the magnetic field,  $S$  is the electronic spin,  $A$  is the contact interaction,  $g$  is the  $g$  factor, and  $r$  is the distance of cobalt to nucleus. The values of  $\omega_e$ ,  $g$ ,  $A$ ,  $D$ , and  $C$  are dependent on the orientation of the complex.

When the dipolar contribution dominates, the relaxation rate is proportional to  $1/r^6$  and can therefore be used to study the geometry of the complex.

**(b) The Rotating Complex.** We consider a complex in solution, with typical molecular rotation times in the range of  $10^{-10}$  to  $10^{-8}$  s. The isotropic part of the contact interaction gives rise to a contact shift

$$\Delta\omega_c = -(A/\hbar)g\beta S(S+1)B/3kT \quad (5)$$

where  $A$  now stands for the isotropic part of the contact interaction and  $g$  is a suitable average of the  $g$ -factor principal values:  $g = 2.8$ .<sup>5</sup>

The isotropic part of the dipolar interaction gives a pseudocontact shift. For complexes which have an axial symmetry

$$\Delta\omega_{pc} =$$

$$\omega_I(g_{\parallel}^2 - g_{\perp}^2)\beta^2 S(S+1)(3 \cos^2 \theta - 1)/[9kT(4\pi\epsilon_0 c^2 r^3)] \quad (6)$$

where  $r$  is the distance of cobalt to nucleus and  $\theta$  the angle between the vector  $\vec{r}$  and the  $g$  symmetry axis.

The sign of the contact shift depends only on the chemical linkage. It is to low field for phosphorus and for the aromatic H8 proton. The pseudocontact shift is of either sign, depending on the value of  $(3 \cos^2 \theta - 1)$ .

The anisotropic parts of the interactions, modulated by molecular rotation, give rise to nuclear relaxation, at rates proportional to the square of  $\langle S_z \rangle$  (the so-called Curie spin mechanism).<sup>13</sup>

**(c) Observability of the Complex.** Due to the shortness of the electronic relaxation time  $\tau_e$ , nuclear relaxation in the static complex (eq 1 and 2) is not very fast. For instance, if  $A/\hbar = 2.7 \times 10^7$  rad/s, a value corresponding to a -2000-ppm shift for phosphorus, and if  $\tau_e = 5 \times 10^{-13}$  s, the contribution to the transverse relaxation rate is only 510 Hz. An equal dipolar contribution is obtained at a distance of 0.21 nm.

In a field of 6.3 T, and using a rotational correlation time of  $10^{-9}$  s, the Curie spin contribution remains smaller than the standard dipolar one.

Thus, the complex should exhibit rather narrow lines, as is indeed found to be the case. In practice, the main contribution to transverse relaxation is due to exchange.

**(2) Complexes in Chemical Exchange.** The following results obtain from the analysis of Swift and Connick.<sup>14</sup>

**(a) Spectrum of the Complex in Slow Exchange.** Let  $\Delta\omega_M = \Delta\omega_c + \Delta\omega_{pc}$  be the paramagnetic shift of a ligand nucleus and  $\tau_M$  be the lifetime of the complex. If  $\Delta\omega_M \tau_M \gg 1$ , the complex resonance is observed as it would be in the absence of exchange, except for lifetime broadening, by an amount  $1/\tau_M$ .

**(b) Spectrum of the Free Ligand Exchanging with a Single Complex.** Let  $f$  be the fraction of complexed ligand and  $T_{1M}$  and  $T_{2M}$  its relaxation times. The chemical exchange between complex and free ligand gives rise to a shift ( $\Delta\omega_p$ ) and to relaxation ( $T_{2p}$ ,

(5) Shulman, R. G.; Sternlicht, H.; Wyluda, B. J. *J. Chem. Phys.* **1965**, *43*, 3116-3122.

(6) Dwek, R. A. *Nuclear Magnetic Resonance in Biochemistry*; Clarendon Press: New York, 1973; p 275-278.

(7) Levy, G. C.; Dechter, J. J. *J. Am. Chem. Soc.* **1980**, *102*, 6191-6196.

(8) Leroy, J. L.; Guéron, M. *Biochimie* **1981**, *63*, 815-819.

(9) Leroy, J. L.; Guéron, M. *Biochimie* **1982**, *64*, 297-299.

(10) Guéron, M.; Weisbuch, G. *J. Phys. Chem.* **1981**, *85*, 517-525.

(11) Bloembergen, N.; Morgan, L. O. *J. Chem. Phys.* **1961**, *34*, 842-850.

(12) Solomon, I. *Phys. Rev.* **1955**, *99*, 559-565.

(13) Guéron, M. *J. Magn. Reson.* **1975**, *19*, 58-66.

(14) Swift, T. J.; Connick, R. F. *J. Chem. Phys.* **1962**, *37*, 307-320.

$T_{1p}$ ) of each line of the original free-ligand spectrum. The lines are henceforth designated as originating from a "free/exchanging" species. For  $T_{2M}$  and  $T_{1M} > \tau_M$ , a condition satisfied in the present experiments, one has

$$\Delta\omega_p = f\Delta\omega_M / (1 + \Delta\omega_M^2\tau_M^2) \quad (7)$$

$$1/T_{2p} = f/T_{2M} + f\tau_M\Delta\omega_M^2 / (1 + \Delta\omega_M^2\tau_M^2) \quad (8)$$

$$1/T_{1p} = f/T_{1M} \quad (9)$$

In the limit of slow exchange ( $\tau_M\Delta\omega_M \gg 1$ ), one has lifetime broadening,  $1/T_{2p} = f/\tau_M$ , and very little shift,  $\Delta\omega_p = f/(\Delta\omega_M\tau_M^2)$ .

In the opposite limit of fast exchange, the resonance lines of the complex and of the free ligand merge at the weighted average of their original positions:  $\Delta\omega_p = f\Delta\omega_M$ . The transverse relaxation rate is  $1/T_{2p} = f\Delta\omega_M^2\tau_M$ .

In all cases and whatever the value of  $f$ , the following relation holds between the observable parameters  $\Delta\omega_p$  and  $T_{2p}$ :

$$\Delta\omega_p T_{2p} = 1 / (\Delta\omega_M\tau_M) \quad (10)$$

If the bound species is observed,  $\Delta\omega_M$  may also be measured. The variation of  $(\Delta\omega_p T_{2p} \Delta\omega_M)^{-1}$  (equal to  $\tau_M$  by eq 10) vs. temperature is expected to follow an activation energy law.

(c) **The Free Ligand in Exchange with Two Complexes.** There are two limiting cases. If the two complexes exchange directly between themselves at a sufficiently large rate, they have the same effect as a single species on the spectrum of the free/exchanging ligand. The other limiting case assumes that the two complexes do not exchange directly at all, and this is the one that we consider.

The contributions of the two complexes are additive. Equations 7–9 are replaced by

$$\Delta\omega_p = \frac{f_A \Delta\omega_{MA}}{(1 + \Delta\omega_{MA}^2 \tau_{MA}^2)} + \frac{f_B \Delta\omega_{MB}}{(1 + \Delta\omega_{MB}^2 \tau_{MB}^2)} \quad (11)$$

$$1/T_{2p} = \frac{f_A \tau_{MA} \Delta\omega_{MA}^2}{(1 + \Delta\omega_{MA}^2 \tau_{MA}^2)} + \frac{f_B \tau_{MB} \Delta\omega_{MB}^2}{(1 + \Delta\omega_{MB}^2 \tau_{MB}^2)} \quad (12)$$

$$1/T_{1p} = f_A/T_{1MA} + f_B/T_{1MB} \quad (13)$$

where  $f_A$  and  $f_B$  are the relative concentrations of the two complexes, A and B.

An interesting feature of these relations is that one complex may provide the main contribution to the shift and/or line broadening at one temperature, whereas the other complex dominates at another temperature. For instance, if both complexes are in fast exchange, the shift of the free/exchanging spectrum is mainly due to the complex with the large shift, assuming the two complexes are in equal numbers. At a lower temperature, the complex with the large shift may have entered the slow exchange regime, and the observed shift is then due to the small-shift complex. Furthermore, at a given temperature, it may happen that one complex is responsible for most of the shift, whereas the other complex dominates broadening. Such behavior could be studied by the variation of the product  $\Delta\omega_p T_{2p}$  vs. temperature, and examples will be found in the Results.

## Materials and Methods

**Preparation of Samples.** 5'-AMP and 5'-CMP were purchased from Sigma Chemical Co. They were dissolved in a solution containing 10%  $\text{D}_2\text{O}$  and passed through a column of Chelex-100 (Biorad) before use. Concentration of nucleotides was measured according to their extinction coefficient:  $\epsilon^{260} = 15400$  for AMP and  $\epsilon^{280} = 9000$  for CMP.<sup>15</sup> Cobalt chloride was added from stock solutions titrated by comparison to a certified standard with use of flame spectroscopy. The sample pH was adjusted as indicated with 0.1 M NaOH or HCl.

For proton NMR, the samples were dissolved in  $\text{D}_2\text{O}$ , passed through Chelex, lyophilized, and redissolved in 99.98%  $\text{D}_2\text{O}$ .  $\text{CoCl}_2$  was added from  $\text{D}_2\text{O}$  solutions.

(15) Handbook of Biochemistry and Molecular Biology, Physical and Chemical Data, 3rd ed.; Fassmann, G. D., Ed.; Chemical Rubber Co.: Cleveland, OH.

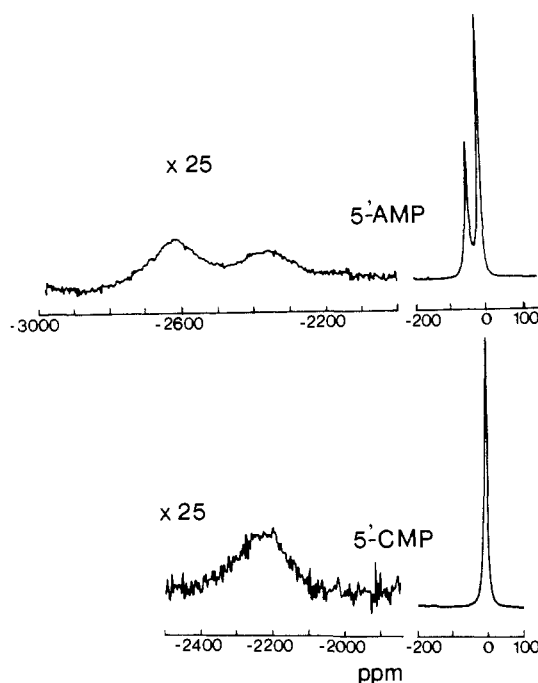


Figure 1. Phosphorus NMR spectra of aqueous cobalt-5'-AMP and cobalt-5'-CMP solutions at  $-10^\circ\text{C}$ . AMP or CMP, 0.3 M; cobalt chloride, 0.1 M; pH 7.4.

The nucleotide concentrations were in the range of 0.06–0.3 M. At these concentrations, the free fraction of cobalt ions may be neglected.

The cobalt complexes are poorly soluble, particularly at high temperatures. At  $4^\circ\text{C}$ , samples whose composition was 0.1 M  $\text{CoCl}_2$  and 0.3 M nucleotide could be conserved for a few hours. For experiments carried out below  $0^\circ\text{C}$ , the samples were filtered through a 0.22- $\mu\text{m}$  Millipore filter and could be kept liquid for at least 1 h at  $-10^\circ\text{C}$ .

**NMR Methods.** The NMR measurements were carried out with a home-made spectrometer operating at 6.48 T.<sup>16</sup> The samples were contained in 8-mm-o.d. microcells for the  $^{31}\text{P}$  measurements and in 5-mm-o.d. NMR tubes for the  $^1\text{H}$  measurements. The frequency scale of  $^{31}\text{P}$  is referred to  $\text{H}_3\text{PO}_4$  (85%) and that of protons to 2,2-dimethylsilapentane-5-sulfonate, whose frequencies are computed by reference to the frequency of the  $\text{D}_2\text{O}$  deuterium lock signal. Transverse relaxation was determined from the line broadening upon addition of Co by the relation  $1/T_{2p} = \pi\Delta$  where  $\Delta$  is the increase of full line width at half-height. Longitudinal relaxation was measured by the inversion-recovery method. Paramagnetic shifts were computed as the difference between the resonance frequencies measured in the presence and absence of  $\text{Co}^{2+}$  with  $\text{D}_2\text{O}$  as the internal reference. The deuterium shift of  $\text{D}_2\text{O}$  could be neglected for this measurement. In some cases, this was checked by using trimethyl phosphate (5 mM) as an internal reference.

The  $^{31}\text{P}$  spectral region was explored between  $-3000$  and  $+1000$  ppm, in frames of 2000 ppm. For intensity comparison, the magnetic field was varied in order to bring successively the lines of interest to the center of the spectral frame, the excitation frequency remaining constant. The length of a  $\pi/2$  pulse was 20  $\mu\text{s}$ .

## Results

At low temperatures ( $-10^\circ\text{C} < T < 20^\circ\text{C}$ ), we observe the phosphorus and proton spectra of bound complexes. These results are described in section A below and demonstrate the existence of more than one complexed species.

At higher temperatures ( $20^\circ\text{C} < T < 95^\circ\text{C}$ ), the solubility of the complexes is low. We therefore look at the nucleotides in the presence of small quantities of cobalt and measure shifts and relaxation of the free/exchanging species (sections B and C). The results demonstrate that in this temperature range also there exists at least two different complexes.

(A) **Direct Observation of Cobalt-Nucleotide Complexes at Low Temperature.** (1) **The Phosphorus Spectrum of Co-5'-AMP Complexes.** The phosphorus spectrum of a sample containing 5'-AMP (300 mM) and cobalt chloride (100 mM) at  $-10^\circ\text{C}$  is

(16) Caron, F.; Guéron, M.; Nguyen, Ngoc Quoc Thuy; Herzog, R. *Rev. Phys. Appl.* **1980**, *15*, 1267–1274.

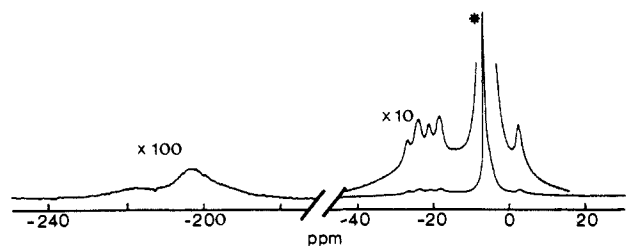


**Figure 2.** Proton NMR spectrum of a solution of 5'-AMP (100 mM) and of cobalt chloride (50 mM).  $T = -10\text{ }^{\circ}\text{C}$ ;  $\text{D}_2\text{O}$ , 99.95%; pH 7.4. The resonance of contaminant HDO partially overlaps the exchange-broadened resonances of free/exchanging AMP.

shown in Figure 1. Four lines are observed, at  $-5$ ,  $-50$ ,  $-2350$ , and  $-2600$  ppm. Comparison with a sodium-AMP sample shows that the total intensity corresponds to all the phosphorus nuclei (300 mM).

On this basis, the  $-5$ -ppm line corresponds to 200 mM. We assign it to the free/exchanging species, broadened and shifted (0.6 ppm downfield from the diamagnetic position) by chemical exchange with Co-AMP complexes.

The other three lines are assigned to cobalt complexes. Their intensities are ca. 80, 7, and 13 mM.

These observations suggest that at least three different complexes are present, the phosphorus-to-cobalt ratio of each being 1:1.

As the temperature is increased, the two low-field lines broaden and merge, as do the high-field lines, due very probably to exchange.

In earlier experiments,<sup>9</sup> we failed to observe any line in the  $-2000$ -ppm region, due most probably to inadequate equipment. At  $5\text{ }^{\circ}\text{C}$ , a  $-2470$ -ppm line has been observed by A. McLaughlin (private communication).

From the shifts of the low-field lines, one derives hyperfine constants of  $2.8 \times 10^7$  and  $3.1 \times 10^7$  rad/s. These values may be compared to those found in crystalline  $\text{Co}_3(\text{PO}_4)_2$ , ca.  $2 \times 10^7$  rad/s.<sup>17</sup> They suggest that the low-field lines are those of complexes whose phosphate group is bound directly to cobalt. The  $-50$ -ppm line presumably belongs to a phosphate bound in an outer-sphere complex.

The closeness of the chemical shifts of the two low-field lines suggests that they originate from structurally related complexes. As pointed out earlier,<sup>9</sup> the  $-50$ -ppm line has an anomalous shape. This suggests that here also two related complexes may be involved. This interpretation is supported by the proton NMR data.

**(2) The Proton Spectrum of Co-5'-AMP Complexes.** The proton spectrum of a sample containing 5'-AMP (100 mM) and cobalt chloride (50 mM) at  $-10\text{ }^{\circ}\text{C}$  is shown in Figure 2. The unresolved region from  $-7$  to  $-2$  ppm includes a residual HDO line as well as exchange-broadened lines at, or close to, the positions in the free AMP spectrum. The other lines are ascribed to cobalt-5'-AMP complexes. The low-field lines at  $-204$  and  $-218$  ppm disappear when H8 is replaced by deuterium and are therefore assigned to H8. The line at 2.8 ppm is assigned to H2 by comparison with spectra of the free/exchanging species, taken in the fast exchange regime (cf. Figure 5), where H2 is the only line to shift toward high field. The remaining lines around  $-20$  ppm should be those of the ribose protons.

The intensities of both the H8 and H2 lines correspond to a concentration of ca. 50 mM, that is, to 100% of the cobalt-complexed AMP if the stoichiometry is one-to-one. The figure of 100% is approximate. It is based on integration of the broad low-field peaks (Figure 2), by comparison with the H8 resonance of an AMP sample devoid of cobalt (not shown). This value may be in error by 30%. The lines around  $-20$  ppm have comparable intensity.

On the basis of intensities, we assign all lines of the proton spectrum to the complex whose phosphorus resonance is at  $-50$  ppm (outer-sphere binding), i.e., the one which accounts for 80%

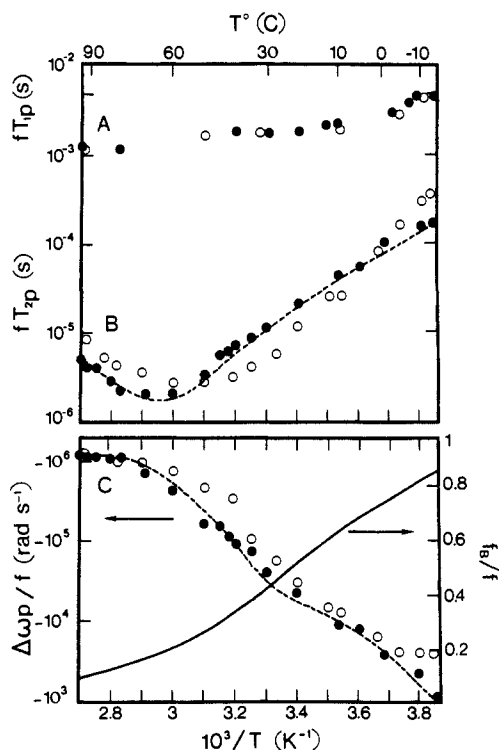


**Figure 3.** Cobalt-induced longitudinal relaxation (A), transverse relaxation (B), and shift (C) of phosphorus in 5'-AMP (●) and 5'-CMP (○). Nucleotide concentration, 60 mM. Relaxation rates and shifts increase linearly with the  $\text{Co}^{2+}$ /nucleotide ratio which varied from  $5 \times 10^{-4}$  to 0.3. In C, the full line is a plot of the proportion,  $f_B/f$ , of the AMP complex B (right-hand scale). The computed values of shifts and relaxation rates (dashed lines) and of  $f_B/f$  are derived from the same fit which also yields the parameters of Table I. All computed lines refer to AMP (●).

of the cobalt-complexed AMP. The large shift of the H8 proton suggests a direct bond between cobalt and N7. We observe that this shift is much larger than the shift of the pyridine  $\alpha$  protons,  $-32.9$  ppm, in the bis-pyridine adduct of  $\text{Co}^{2+}$ -acetylacetonate,  $\text{Co}(\text{acac})_2(\text{pyridine})_2$ .<sup>18</sup> The existence of two H8 lines again suggests that the complex in fact corresponds to two related species.

The proton lines of the complexes responsible for the phosphorus low-field lines should be less intense and less shifted (see section C1), and therefore difficult to detect. They are not observed.

**(3) The Phosphorus Spectrum of Co-5'-CMP Complexes.** The CMP spectrum, shown in Figure 1, should be compared with that of AMP. The concentration of CMP is 300 mM, and that of cobalt is 100 mM.

The intensity of the  $-2220$ -ppm line corresponds to 30 mM and that of the  $-4$ -ppm line to 270 mM. This spectrum is analogous to that of AMP, and we assume that it corresponds to the same situation: the low-field line is that of an inner-sphere phosphate-cobalt complex. The line at high field results from fast exchange (vs. slow exchange for AMP) between free CMP and an outer-sphere phosphate-cobalt complex whose concentration is 70 mM. This interpretation is supported by measurements at different cobalt and CMP concentrations, which show that the relative intensities of the two lines, and their shifts, are a function only of the cobalt/CMP ratio. On the basis of the observed shift of the high-field resonance, the paramagnetic shift of this outer-sphere complex is negative and smaller than 6 ppm.

We were unable to observe the proton spectrum of any CMP complex, probably because the condition  $\Delta\omega_M\tau_M > 1$  is not fulfilled, even at  $-10\text{ }^{\circ}\text{C}$ .

**(B) Demonstration of Multiple Complexation at Higher Temperatures (Free/Exchanging Situation).** **(1) Phosphorus Shifts and Transverse Relaxation.** The data are presented in Figure 3. Qualitatively, they suggest a situation of fast exchange at high

(17) Mays, J. M. *Phys. Rev.* **1957**, *108*, 1090-1091.

(18) Horrocks, W. D.; Taylor, R. C.; La Mar, G. N. *J. Am. Chem. Soc.* **1964**, *86*, 3031-3038.

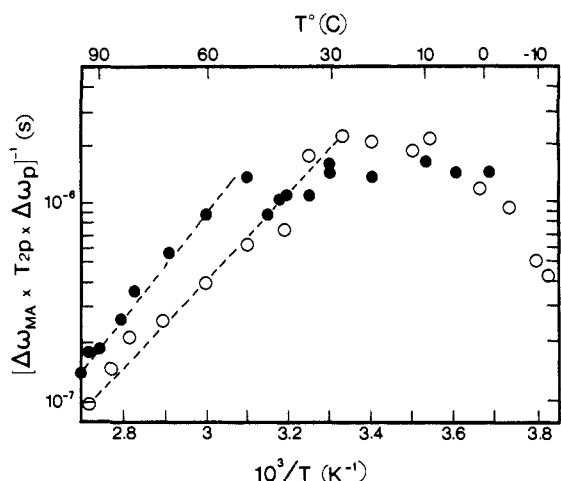


**Figure 4.** Plot of  $[T_{2p}\Delta\omega_p\Delta\omega_{MA}]^{-1}$  vs.  $1/T$  for phosphorus. If A were the only complex, this product would be equal to its lifetime  $\tau_{MA}$ , and its temperature variation would be linear in the semilog plot. This is the case at high temperature (dashes) for both 5'-AMP (●) and 5'-CMP (○). The curvature of the plot at lower temperatures shows that shift and transverse relaxation are controlled by exchange with different complexes. The data are those of parts B and C in Figure 3. The phosphorus paramagnetic shifts at  $-10^\circ\text{C}$  are  $\Delta\omega_{MA} = -2530$  ppm for AMP and  $-2220$  ppm for CMP. The values at other temperatures are computed by eq 5.

temperature. The increased  $T_2$  and decreased shift at low temperature would be due to slow exchange. We shall see that this model holds only for temperatures above  $40^\circ\text{C}$ .

If there were a single complex, we could obtain its lifetime from relation 10. The value of  $1/\Delta\omega_p T_{2p} \Delta\omega_M$  vs.  $1/T$  is plotted in Figure 4. The linear plot at high temperatures shows that relaxation and shift are indeed dominated by exchange with a single complex whose lifetime has an activation energy of  $50$  kJ/mol for the AMP complex, and  $42$  kJ/mol for the CMP complex. These values are obtained independently of the value of  $f$ , even if  $f$  varies with temperature due to the existence of another complex.

It is clear from Figure 4 that the single-complex model does not hold at lower temperatures, since the plot is no longer linear. In Figure 3, one sees that the shift diminishes more slowly than expected for a single complex, as the temperature is reduced.

The temperature dependence of the shift is readily explained if one introduces a second complex, whose shift is smaller than the shift of the first complex, and which is still in fast exchange at temperatures low enough for the first one to be in slow exchange.

**(2) Proton Shifts and Transverse Relaxation of 5'-AMP.** The shifts for different temperatures are reported in Figure 5.

When the temperature increases, from  $-10$  to  $30$  or  $40^\circ\text{C}$ , the shifts increase as expected if one goes from a slow-exchange regime (eq 7). However, the reduction of the shift at higher temperatures cannot be explained by exchange with a single complex whose fractional population  $f$  would be independent of temperature. Dissociation at higher temperatures could explain a reduced shift. However, the reductions for the different protons would be expected to be in the same ratio, contrary to observation.

Hence the data demonstrate that two complexes at least are present in the range of temperatures considered here.

The existence of a minimum in the plot of  $fT_{2p}$  vs. temperature (Figure 6) shows that transverse relaxation enters the fast-exchange regime between  $10^\circ\text{C}$  (for ribose protons) and  $30^\circ\text{C}$  for H8.

**(C) Interpretation in Terms of Two Complexes. (1) Paramagnetic Shifts and Transverse Relaxation: Fractional Concentrations of the Two Complexes.** The data of Figures 3–6 may be interpreted in terms of two complexes, A and B. Complex A is the phosphate-to-cobalt innersphere complex. Its phosphorus paramagnetic shift is obtained from the low-temperature spectrum (Figure 1), in which we ignore the distinction between the  $-2350$ - and  $-2620$ -ppm lines and consider instead a complex having the

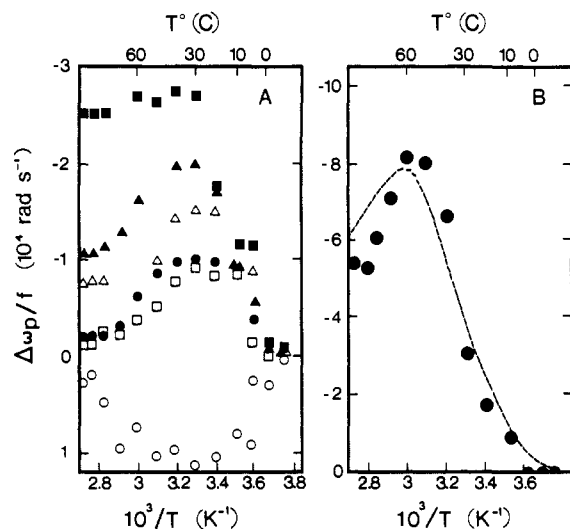


**Figure 5.** Proton shifts of free/exchanging AMP, induced by exchange with AMP complexed to  $\text{Co}^{2+}$ . Panel A: H2 (○), H1' (□), H2' (●), H3' (Δ), H4' (▲), and H5' (■); all protons shift downfield except H2. In panel B, the shift of H8 (●) is fitted according to eq 5 and 11 with the parameters of Table I. The ratio of cobalt to AMP varied from  $10^{-3}$  to  $5 \times 10^{-2}$ ; AMP,  $0.1$  M; pH  $7.4$ ;  $\text{D}_2\text{O} = 99.98\%$ .

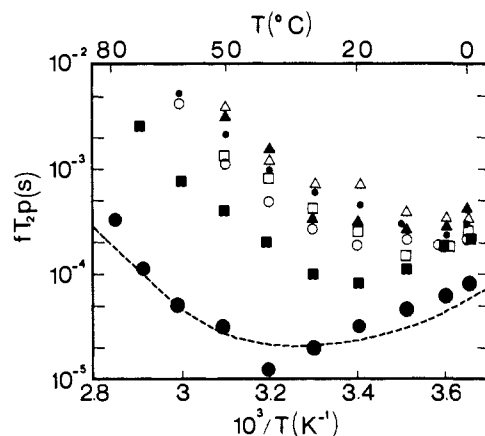


**Figure 6.** Cobalt-induced transverse relaxation of 5'-AMP protons. Same symbols and experimental conditions as in Figure 5. The dashed line for the transverse relaxation time of proton H8 is computed from eq 5 and 12 with the parameters of Table I.

weighted average shift  $\Delta\omega_{MA} = -2530$  ppm at  $-10^\circ\text{C}$ . Complex B is the phosphate outersphere complex with  $\Delta\omega_{MB} = -48$  ppm at  $-10^\circ\text{C}$ .

Assuming that paramagnetic shifts are proportional to  $1/T$ , complex A would be shifted by  $\Delta\omega_{MA} = -1808$  ppm at  $95^\circ\text{C}$ . The large shift measured at  $95^\circ\text{C}$  ( $\Delta\omega_p/f = -1780$  ppm) shows that this complex is the majority species at high temperature. It should then dominate the line-broadening process.

Knowing the value of  $\Delta\omega_{MA}$ , as well as the measured shift and broadening of the free/exchanging species (Figure 3), we obtain the lifetime  $\tau_{MA}$  from eq 10 for all temperatures between  $50$  and  $95^\circ\text{C}$ , where shift and relaxation are dominated by exchange with complex A. In this temperature range,  $\tau_{MA}$  can be read off directly from Figure 4. From  $\tau_{MA}$ , we next obtain via eq 7 and 8 the fraction  $f_A$  of complex A.

The values of  $f_A$  and  $f_B$  are also known at  $-10^\circ\text{C}$  on the basis of the phosphorus spectra of the bound species such as Figure 1. They should obey the relations

$$f_A + f_B = f$$

$$f_A/f_B = \exp[-(\Delta H/kT)] \exp(\Delta S/k)$$

where  $\Delta H$  and  $\Delta S$  are the differences in enthalpy and entropy between complexes A and B. Both the high- and low-temperature

**Table I.** Thermodynamic and Kinetic Parameters and Paramagnetic Shift of Co-AMP and Co-CMP Complexes, Obtained by Fitting the Experimental Data to Equations 7 and 8

complex		$\tau_M^{295, a}$ $\mu\text{s}$	$E_{\text{act}}^b$ kJ/mol	$\Delta H^c$ kJ/mol	$\Delta S^c$ kJ/mol/K	$\Delta\omega_M^{263}$ , ppm	
						$^{31}\text{P}$	$^1\text{H8}$
AMP	A	10	50	31	31/295	-2530 <sup>d</sup>	-37 <sup>e</sup>
	B	15	41			-48 <sup>d</sup>	-203 <sup>d</sup>
CMP	A	30	42	19	19/295	-2220 <sup>d</sup>	
	B					<-6	

<sup>a</sup>Complex lifetime at 295 K. <sup>b</sup>Activation energy for dissociation of the complex. <sup>c</sup>These values are derived from the relative concentrations  $f_A$  and  $f_B$  of the two complexes:  $f_A/f_B = \exp[-(\Delta H/kT)] \exp(-\Delta S/k)$ . Note that  $f_A = f_B$  at 295 K (22 °C). <sup>d</sup>Values obtained from the low-temperature spectra of the complexes (Figures 1 and 2). <sup>e</sup>The paramagnetic shift of H8 in complex A was obtained as an adjustable parameter from the fits presented in Figures 5 and 6.

data can be fitted with  $\Delta S = 31/295$  kJ/(mol·°C) and  $\Delta H = 31$  kJ/mol for AMP and with  $\Delta S = 19/295$  kJ/mol/K and  $\Delta H = 19$  kJ/mol for CMP. The proportion  $f_B/f$  of the B species of Co-5'-AMP is plotted in Figure 3C.

Below 10 °C, the exchange with complex A is too slow to contribute to the shift of the  $^{31}\text{P}$  free/exchanging resonance (Figure 3). The shift is dominated by exchange with complex B. On the basis of eq 7 and using the fractional occupation  $f_B$ , we determine from  $^{31}\text{P}$  shifts measured between -10 and 10 °C the lifetime  $\tau_{MB}$  of this complex. The temperature dependence corresponds to an activation energy of 41 kJ/mol.

With use of the activation energies, the lifetime of both complexes can be computed over the entire temperature range. Together with the shifts and occupancies of the complexes, they enable us to predict the line width and shift of the  $^{31}\text{P}$  resonance of free/exchanging AMP between -10 and 95 °C. Good agreement with experimental data is obtained as shown in Figure 3 where the dashed lines are computed. The spectroscopic, thermodynamic, and kinetic parameters are given in Table I.

The H8 shifts and transverse relaxation rates are also interpreted in terms of complexes A and B. This is shown in Figures 5 and 6, where the dashed lines are computed with the kinetic and thermodynamic parameters just described. The required value of  $\Delta\omega_{MA}$  for H8, which is unknown, was chosen to give the best fit:  $\Delta\omega_{MA} = -37$  ppm at -10 °C. At intermediate temperatures, the H2 shift (Figure 5) is somewhat larger than predicted.

**(2) Longitudinal Relaxation Times.** Turning to longitudinal relaxation, we first consider phosphorus (Figure 3A). With an electronic relaxation time  $\tau_e$  of  $5 \times 10^{-13}$  s, the relaxation rate  $1/T_{1M}$  due to the contact interaction in the innersphere complex "A", given by eq 1, is  $880 \text{ s}^{-1}$ . The dipolar contribution at 0.3 nm, a typical distance for an innersphere complex, would be somewhat smaller ( $200 \text{ s}^{-1}$ ). At high temperature,  $^{31}\text{P}$  relaxation is due mainly to the innersphere complex which is the majority species and also the most efficient for relaxation, by virtue of its large contact and dipolar interactions. The comparison of the lifetime of the complex (Figure 4) with  $fT_{1p}$  (Figure 3A) shows that the regime is fast exchange, and the value of  $fT_{1p}$  is indeed close to 1 ms as expected. At lower temperature, the inner sphere complex, whose fractional occupancy is never smaller than 20%, should continue to dominate longitudinal relaxation of the free/exchanging species, as long as the fast-exchange regime applies. This is the case over the entire temperature range.

The modest reduction of the relaxation rate at low temperature results from two effects: first, the reduced fraction of the complex in form A; second the increased electronic spin relaxation time  $\tau_e$  of cobalt at low temperatures, which would tend to increase nuclear relaxation rates at low temperature. An increase of  $\tau_e$  by a factor of 2 at the lower temperatures is independently suggested by the temperature dependence of proton relaxation of cobalt complexes such as  $\text{Co}(\text{H}_2\text{O})_6^{19}$  and  $\text{Co}(\text{CH}_3\text{OH})_6^{20}$  where

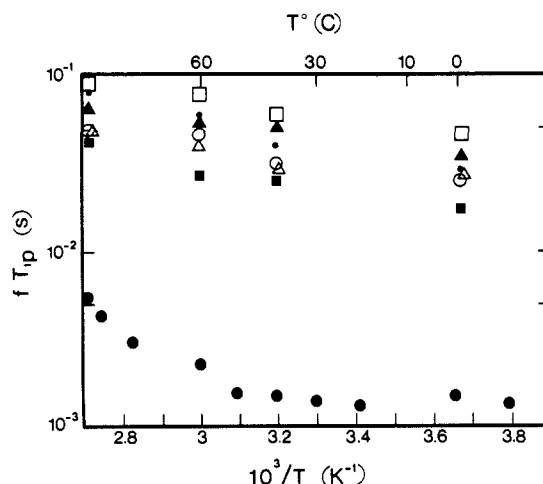


**Figure 7.** Cobalt-induced longitudinal relaxation of 5'-AMP protons. Same symbols and experimental conditions as in Figure 5. The relaxation times of H2 and ribose protons vary with temperature like that of water protons in aqueous solutions of  $\text{Co}^{2+}$ .<sup>19</sup> It is therefore supposed that this variation reflects the temperature dependence of the cobalt electronic relaxation time. By scaling the proton-to- $\text{Co}^{2+}$  distance from  $T_{1p}$  measured for water protons and using the values of  $f_B/f$  shown in Figure 5C, we find the following Co-H8 distances: 0.37 nm in complex A and 0.32 nm in complex B.

the cobalt-to-proton distance should be temperature independent. The proton relaxation rates in these complexes vary much as those of the ribose protons of 5'-AMP (Figure 7).

At -10 °C, as observed previously, the  $^{31}\text{P}$  relaxation rates of the free/exchanging AMP line at -5 ppm and of the outersphere complex line at -50 ppm (Figure 1) are equal, because they are in mutual fast exchange.<sup>9</sup> Their relaxation is caused by exchange with the innersphere complex.

The H8 proton relaxation rate is much increased at low temperatures (Figure 7). The -203-ppm contact interaction is too small to account for the observed rates. For H8 as for all other protons, at all temperatures, longitudinal relaxation is therefore due to the dipolar interaction.

Assuming the same cobalt relaxation time  $\tau_e$  as in the hexahydrate complex, in which the cobalt-to-proton distance is 0.28 nm,<sup>21</sup> and using the values of  $f_A/f_B$  determined above, we find distances from cobalt to H8 of 0.37 nm in complex A and 0.32 nm in complex B.

At intermediate temperatures, the fit with the fractional values  $f_B$  of Figure 3C is poor.

**(D) Optical Spectra.** Cobalt(II) can form both octahedral and tetrahedral complexes. We have measured the spectra of the low-temperature complexes of 5'-AMP and 5'-CMP and compared them with the spectra of octahedral and tetrahedral complexes.<sup>22</sup> The experiments were done at 5 °C, in solutions containing 0.1 M cobalt chloride and 0.2 M nucleotide.

Precipitation of the complex forbade studies at high temperatures.

The spectrum of Co-5'-AMP has the same shape as that of octahedral cobalt hexahydrate. Its extinction coefficient is twice as large:  $\epsilon_{\text{max}}^{510} = 1.05$ .

The spectrum of Co-5'-CMP is slightly shifted from that of Co-5'-AMP, with the maximum at 520 nm ( $\epsilon_{\text{max}}^{520} = 0.98$ ). Weak bands at 565, 590, and 610 nm could be ascribed to a tetrahedral complex. Their intensity would correspond to a proportion of 1%, given the  $\epsilon$  values ( $\epsilon_{\text{max}} \approx 100$ ) measured for such complexes.<sup>22</sup> The tetrahedral complex can therefore be ignored in the analysis of the NMR data.

Since the high-temperature complex is present even at low temperatures, these results indicate that complexes A and B are both octahedral.

(19) Bernheim, R. H.; Brown, T. H.; Gutowsky, H. S.; Woessner, D. E. *J. Chem. Phys.* **1959**, *30*, 950-956.

(20) Luz, Z.; Meiboom, S. *J. Chem. Phys.* **1964**, *40*, 1058-1066.

(21) Morgan, L. O.; Nolle, A. W. *J. Chem. Phys.* **1959**, *31*, 365-368.

(22) Ballhausen, C. J.; Jorgensen, C. K. *Acta Chem. Scand.* **1955**, *9*, 397-403.

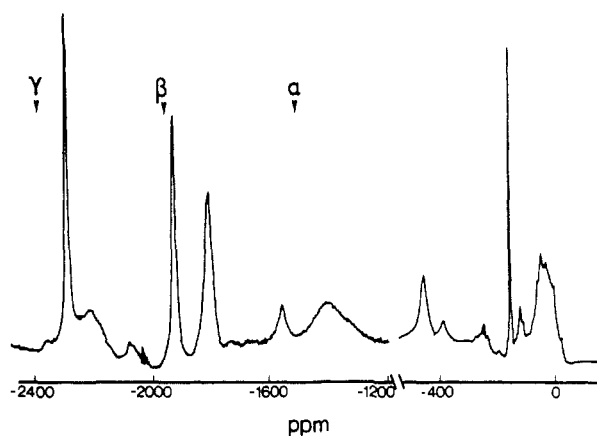


**Figure 8.** The  $^{31}\text{P}$  spectrum of a solution of 5'-ATP (100 mM) and  $\text{CoCl}_2$  (105 mM) at  $-10\text{ }^\circ\text{C}$ , pH 7.0. Arrows indicate the expected resonance frequencies of the  $\alpha$ ,  $\beta$ , and  $\gamma$  phosphates on the basis of the data obtained in the fast-exchange regime at  $90\text{ }^\circ\text{C}$ .<sup>26</sup> Different ATP concentrations were tested in the range 50–300 mM, using the same  $\text{Co}^{2+}$ -to-ATP ratio. All gave the same spectrum.

### Discussion

The main result of this study is the observation and characterization of different complexes of cobalt with mononucleotides, in the slow-exchange regime. The equilibrium between these complexes is temperature dependent. All the complexes are octahedral.

**(a) High-Temperature Complexation.** In the high-temperature complex, "A", of 5'-AMP, the phosphorous shift ( $\Delta\omega_p/f = -1780$  ppm at  $95\text{ }^\circ\text{C}$ ) indicates that  $\text{Co}^{2+}$  is directly bound to phosphate. The small shift of H8 ( $\Delta\omega_p/f = -29$  ppm at  $95\text{ }^\circ\text{C}$ ) and the H8-to- $\text{Co}^{2+}$  distance (0.37 nm) are consistent with ligation to N7 through a water molecule. The proportion of this species increases from 20% for Co-5'-AMP (and 30% for Co-5'-CMP) at  $-10\text{ }^\circ\text{C}$  to about 50% at  $22\text{ }^\circ\text{C}$  and nearly 100% at  $95\text{ }^\circ\text{C}$ .

**(b) Low Temperature Complexation of 5'-AMP.** The paramagnetic shifts of H8 ( $\Delta\omega_{\text{MB}} = -203$  ppm at  $-10\text{ }^\circ\text{C}$ ) and phosphorus ( $\Delta\omega_{\text{MB}} = -48$  ppm at  $-10\text{ }^\circ\text{C}$ ) suggest that, in the "B" complex, cobalt is directly coordinated to the nitrogen N7 of the purine ring and binds simultaneously to the phosphate group through a water molecule.

The lifetimes of complexes A and B are comparable in the whole range of temperatures. They are respectively 0.15 and 0.55  $\mu\text{s}$  at  $95\text{ }^\circ\text{C}$  and 150 and 100  $\mu\text{s}$  at  $-10\text{ }^\circ\text{C}$ .

Although it accounts for most of the data, the description in terms of two complexes is an oversimplification: the phosphorus and H8 proton spectra show the existence of two sets of two related complexes, rather than two complexes. One may speculate that each set might consist first of an isolated complex and second of the same complex to which one nucleotide, or more, would be aggregated.

**(c) Low-Temperature Complexation of 5'-CMP.** At  $-10\text{ }^\circ\text{C}$ , 70% of the cobalt bound to 5'-CMP exchanges rapidly on the NMR time scale with the free ligand. Fast exchange precludes a detailed description of the dominant binding mode. Nevertheless, the small shift measured for  $^{31}\text{P}$  ( $\Delta\omega_p \leq -6$  ppm) and the absorbance spectrum of bound cobalt indicate that (i) the metal ion

is not directly bound to phosphate and (ii) its coordination is not tetrahedral.

**(d) Comparison with Crystal Structures.** There are no reports of a crystal structure for Co-5'-AMP. In the crystallized Co-5'-IMP,<sup>23</sup> cobalt coordinates directly to N7 and through water to phosphate. This is the coordination found in the present work for the low-temperature complex "B"; and furthermore the cobalt to H8 distances are the same (0.32 nm).

Conversely, the high-temperature complex, "A", of Co-5'-AMP, in which Co coordinates directly to phosphate, differs from all known crystalline forms of cobalt-5'-purine monophosphates.

For Co-5'-CMP, both solution complexes differ from the crystal form in which cobalt is tetrahedral.

**(e) Other Ligands: ATP, Polynucleotides.** Direct observation of the bound species provides a straightforward demonstration of the existence of different complexes in equilibrium. We present as further illustration the  $^{31}\text{P}$  spectrum of a sample containing 5'-ATP (0.1 M) and  $\text{CoCl}_2$  (0.105 M) at  $-10\text{ }^\circ\text{C}$  (Figure 8). The spectrum shows more than 15 peaks. It is indicative of five different species in equilibrium, including probably dimers<sup>24</sup> and outersphere complexes. The existence of multiple complexes should easily explain the anomalous temperature dependence of the H8, H2, and H1' proton shifts, observed earlier by Sternlicht et al.<sup>25</sup>

Broadening of all the  $^{31}\text{P}$  peaks as temperature is raised demonstrates slow exchange (not shown). Chemical shifts of  $-2308$  and  $-1941$  ppm are close to those of the  $\gamma$  phosphate ( $-2400$  ppm) and of the  $\beta$  phosphate ( $-1960$  ppm) in the first coordination shell of cobalt, as computed from measurements in the fast-exchange regime.<sup>26</sup> From the same assignments, the  $\alpha$  phosphate would be observed at  $-1520$  ppm. The resonances between  $-60$  and  $+16$  ppm may correspond to outersphere complexes. The line at  $-162$  ppm is surprisingly narrow (340 Hz) and indicates a long-lived complex ( $\tau_M = 10^{-3}$  s). The assignment of the peaks of this spectrum and the analysis of the equilibrium between the different species remain undone.

In ribo- and deoxypolynucleotides, magnetic relaxation studies show an increased distance from manganese<sup>8</sup> and cobalt (in preparation) to phosphorus when the temperature is lower than  $60\text{ }^\circ\text{C}$ . Multiple complexation is therefore indicated for these compounds also.

Being both a shift and a relaxation reagent, the  $\text{Co}^{2+}$  ion is a powerful tool for exploring the structure of its complexes. The spectroscopic features of the ion, rather than an exceptional chemistry of its complexes, may be the reason why multiple complexation can be demonstrated. The preference for binding through water at low temperature, observed in the present work, could turn out to be a property of many metal-to-phosphate complexes.

**Registry No.** Co-5'-ATP, 18925-85-4; Co-5'-CMP, 37308-57-9; Co-5'-AMP, 18839-80-0.

(23) Aoki, K. *Bull. Chem. Soc. Jpn.* **1975**, *48*, 1260–1271.

(24) Scheller, K. H.; Hofstetter, F.; Mitchell, P. R.; Prijs, B.; Sigel, H. *J. Am. Chem. Soc.* **1981**, *103*, 247–260.

(25) Sternlicht, H.; Shulman, R. G.; Anderson, E. W. *J. Chem. Phys.* **1965**, *43*, 3133–3143.

(26) Sternlicht, H.; Shulman, R. G.; Anderson, E. W. *J. Chem. Phys.* **1965**, *43*, 3123–3132.